HHS Public Access

Author manuscript

Neurobiol Dis. Author manuscript; available in PMC 2023 January 01.

Published in final edited form as:

Neurobiol Dis. 2022 January ; 162: 105583. doi:10.1016/j.nbd.2021.105583.

KLF15 overexpression in myocytes fails to ameliorate ALS-related pathology or extend the lifespan of SOD1G93A mice

Ryan Massopust[1,*], **Devin Juros**[1,*], **Dillon Shapiro**[2], **Mikayla Lopes**[1], **Saptarsi M. Haldar**[3,4,5], **Thomas Taetzsch**[1], **Gregorio Valdez**[1,6,7]

[1]Department of Molecular Biology, Cell Biology and Biochemistry, Brown University, Providence, Rhode Island, USA

[2]Molecular Biology, Cell Biology, & Biochemistry Graduate Program, Brown University, Providence, Rhode Island, USA

[3]Gladstone Institutes, San Francisco, California, USA

[4]Department of Medicine, Cardiology Division, UCSF School of Medicine, San Francisco, California, USA

[5]Current address: Amgen Research, South San Francisco, California, USA

[6]Center for Translational Neuroscience, Robert J. and Nancy D. Carney Institute for Brain Science and Brown Institute for Translational Science, Brown University, Providence, Rhode Island, USA

[7]Department of Neurology, Warren Alpert Medical School of Brown University, Providence, United States.

Abstract

Amyotrophic Lateral Sclerosis (ALS) is a currently incurable disease that causes progressive motor neuron loss, paralysis and death. Skeletal muscle pathology occurs early during the course of ALS. It is characterized by impaired mitochondrial biogenesis, metabolic dysfunction and deterioration of the neuromuscular junction (NMJ), the synapse through which motor neurons communicate with muscles. Therefore, a better understanding of the molecules that underlie this pathology may lead to therapies that slow motor neuron loss and delay ALS progression. Kruppel Like Factor 15 (KLF15) has been identified as a transcription factor that activates alternative metabolic pathways and NMJ maintenance factors, including Fibroblast Growth Factor Binding Protein 1 (FGFBP1), in skeletal myocytes. In this capacity, KLF15 has been shown to play a

Corresponding Author: Gregorio Valdez, Brown University, 70 Ship St, Providence, RI 02903, gregorio_valdez@brown.edu.
*These authors contributed equally to this work.

Author Contributions

Conceptualization, Methodology, Validation, Supervision, Project Administration, and Writing-Original Draft, G.V. and T.T.; Formal Analysis, G.V., T.T., D.S., D.J., and R.M.; Writing-Reviewing & Editing, G.V., T.T., S.H., D.J. and R.M..; Investigation, T.T., D.S., D.J., and R.M; Data Curation and Visualization, T.T.; Resources, G.V. and S.H.; Funding Acquisition, G.V.

Competing Interest Disclosure

Saptarsi M. Haldar is an executive, officer and shareholder of Amgen and a scientific founder and shareholder of Tenaya Therapeutics.

protective role in Duchenne muscular dystrophy (DMD) and spinal muscular atrophy (SMA), however its role in ALS has not been evaluated. Here, we examined whether muscle-specific KLF15 overexpression promotes the health of skeletal muscles and NMJs in the SOD1^{G93A} ALS mouse model. We show that muscle-specific KLF15 overexpression did not elicit a significant beneficial effect on skeletal muscle atrophy, NMJ health, motor function, or survival in SOD1^{G93A} ALS mice. Our findings suggest that, unlike in mouse models of DMD and SMA, KLF15 overexpression has a minimal impact on ALS disease progression in SOD1^{G93A} mice.

Keywords

KLF15; ALS; NMJ; FGFBP1

Introduction

Amyotrophic Lateral Sclerosis (ALS) is a progressive and fatal neurodegenerative disease that preferentially affects the neuromuscular system. Treatment options are limited and are only able to extend survival by 2–3 months. Thus, there is a pressing need to pursue all possible strategies to develop treatments for ALS [1]. ALS compromises the function and viability of skeletal muscles, motor neurons and the synapse formed between them, the neuromuscular junction (NMJ). Deleterious changes in skeletal muscles are thought to occur prior to symptom onset and have been linked to progressive degeneration of motor neurons [2,3]. In light of this, preserving the function and structure of skeletal muscles may slow NMJ and motor neuron degeneration in ALS.

A number of studies lend support to the possibility that pathological changes in skeletal muscles influence ALS progression. Research in ALS patients and in the SOD1^{G93A} ALS mouse model has shown that progressive degeneration of skeletal muscles [2,3] and their NMJs [4–6] are an early pathological feature of ALS and likely occur prior to motor neuron loss. Overexpression of SOD1^{G93A} or SOD1^{G37R} specifically in skeletal muscles results in muscle atrophy in young adult mice [7–9] and NMJ denervation, motor neuron loss and impaired motor function with increasing age [8,9]. The introduction of these mutant genes specifically into skeletal muscles also alters the morphology and impairs the function of mitochondria, suggesting that metabolic pathways in muscles may be a primary target of ALS pathology [7]. In support of this, skeletal muscles of individuals afflicted with ALS have been reported to exhibit morphological abnormalities in mitochondria [10–13], increased reliance on fatty acid oxidation and other alternative metabolic pathways [14–17]. These changes in skeletal muscle metabolism are in line with dramatic increases in global energy expenditure in ALS patients [18]. As a prominent site of energy usage within the body [19], disruptions in skeletal muscle metabolism are thought to substantially contribute to global hypermetabolism in ALS patients. Therapeutic approaches that target energy availability or metabolism, however, have had mixed success in ALS patients [18], highlighting the need to identify additional metabolic regulators that could influence disease progression.

The transcription factor Kruppel Like Factor 15 (KLF15) is highly expressed in skeletal muscles where it induces gene programs that govern adaptive metabolic pathways in response to changes in the extracellular environment, hormonal cues or physiological stress [20–22]. Skeletal muscle specific *Klf15* deletion in mice impairs muscle lipid metabolism and substantially impacts systemic energy expenditure, body weight and lipid homeostasis in non-muscle tissues [23]. Recent studies in mouse models have demonstrated that KLF15 exerts protective effects in skeletal muscles affected by Duchenne muscular dystrophy (DMD) [22] and has mixed success in improving spinal muscular atrophy (SMA) [24,25]. KLF15 exerts these positive effects through regulation of both metabolic and non-metabolic genes [22]. The latter group includes the secreted fibroblast growth factor binding protein 1 (FGFBP1) [22], which has been shown to prevent NMJ degeneration in $SOD1^{G93A}$ mice [26]. Moreover, KLF15 is enriched in slow twitch skeletal muscles [20], which are resistant to ALS pathology [27]. The involvement of KLF15 in promoting metabolism of alternate nutrients in skeletal muscles, particularly those afflicted by chronic stress such as DMD, and inducing expression of synaptogenic factors such as FGFBP1, suggests that it may serve a protective role in skeletal muscles afflicted by ALS.

In the current study, we asked if KLF15 overexpression in skeletal muscles delays muscle atrophy, loss of motor function, and death associated with ALS. To do so, we crossed the $SOD1^{G93A}$ mouse line, a model of ALS, with a transgenic line in which KLF15 is overexpressed specifically by skeletal muscle fibers. We found that muscle-specific KLF15 overexpression did not prevent muscle atrophy or slow overall disease progression in ALS mice. This may be partly due to the failure of overexpressed KLF15 to increase levels of FGFBP1 and other target genes in skeletal muscles of $SOD1^{G93A}$ mice. These results demonstrate that unlike in DMD and SMA, KLF15 overexpression does not protect skeletal muscles in a mouse model of ALS.

Methods

Animals

$SOD1^{G93A}$ mice [28] were purchased from Jackson Laboratories (RRID:IMSR_JAX:004435, Bar Harbor, ME). KLF15 muscle transgenic mice in a pure C57BL/6J background, which have been described by the laboratories of Saptarsi Haldar and Mukesh Jain [22] (no RRID available), were obtained with permission and herein referred to as MTg. Heterozygous MTg female mice were crossed with heterozygous $SOD1^{G93A}$ male mice to generate wild type (WT), MTg, $SOD1^{G93A}$ and $SOD1^{G93A}$;MTg littermates for experimental comparisons. All mice were maintained on a mixed genetic background. A lethal dose of isoflurane was used to sacrifice mice for tissue collection. Animals were housed in a 12-hour light/dark cycle with access to food and water ad libitum. Breeding, housing, and experimental use of animals were performed in a pathogen free environment in accordance with the National Institutes of Health, Virginia Tech Institutional Animal Care and Use Committee (Protocol# 18-148 and 18-176), and Brown University Institutional Animal Care and Use Committee (Protocol# 19-05-0013) guidelines.

Immunohistochemistry (IHC)

Intracardial perfusion with phosphate buffered saline followed by 4% paraformaldehyde (PFA) was performed on mice prior to collection of tissue for IHC. For analysis of nicotinic acetylcholine receptors (AChRs), the extensor digitorum longus (EDL) muscle was incubated in blocking buffer (5% BSA, 3% goat serum, 0.1% Triton X-100 in PBS) for 1 h at room temperature, Alexa Fluor 488 conjugated alpha-bungarotoxin (Invitrogen #B13422) diluted 1:1000 in blocking buffer for 2h at room temperature, washed 3X in PBS, and whole mounted to a microscope slide in Vectashield (Vector Laboratories, Burlingname, CA). For muscle fiber analysis, the tibialis anterior (TA) muscle was incubated in 30% sucrose diluted in PBS for 48 h at 4°C, mounted in Tissue Freezing Medium (General Data, Cincinnati, OH, #TFM-5), and cross-sectioned at 16 μm with a cryostat. TA cross sections were mounted to gelatin coated microscope slides, washed 3X in PBS, incubated in blocking buffer (5% BSA, 3% goat serum, 0.1% Triton X-100 in PBS) for 1 h at room temperature, incubated in rabbit anti-laminin antibody (Sigma-Aldrich, St. Louis, MO, #L9393, RRID: AB_477163) diluted 1:250 in blocking buffer overnight at 4°C, washed 3X in PBS, incubated in Alexa Fluor 488 conjugated polyclonal goat anti-rabbit IgG (Invitrogen#A-110008, RRID: AB_143165) diluted 1:1000 in blocking buffer for 1 h at room temperature, washed twice in PBS, incubated in DAPI (1:1000 in PBS) for 20 minutes at room temperature, washed twice in PBS, and covered in Vectashield mounting medium (Vector Laboratories, Burlingname, CA).

Imaging

Images were obtained with a Zeiss LSM 710 or Zeiss LSM 900 laser scanning confocal microscope (Carl Zeiss Microscopy, Berlin, Germany) using a 20× (0.8 numerical aperture) objective. Maximum intensity projections and stitching of tile scans were generated with Zeiss Zen software (RRID: SCR_013672).

AChR Analysis

An average of 72 endplates per animal were randomly sampled using the grid overlay function in ImageJ software (RRID:SCR_003070) based on the fractionator method [29] from tile scan images of the EDL muscle in which AchRs were labeled with Alexa Fluor-conjugated alpha bungarotoxin (fBTX). Receptor fragmentation was assessed by counting the number of AChR islands at an individual endplate. ImageJ was used to measure the area of AChR endplates. The genotype and sex of the samples were blinded to the analyst.

Muscle fiber size analysis

Analyses of skeletal muscle fiber minimum Feret's diameter (MFD) and presence of centrally located nuclei were performed on cross sections collected from the medial TA and soleus. Muscle fibers were identified by laminin labeling of the ECM adjacent to the sarcoplasm. Muscle fibers with centrally located nuclei were identified by the presence of one or more DAPI-labeled nuclei within a muscle fiber cross section and not directly touching laminin labeled ECM. An average of 374 muscle fibers per muscle were randomly sampled using the grid overlay function in ImageJ software (RRID:SCR_003070) based on the fractionator method [29]. Muscle fiber minimum Feret's diameter measurements and

counting of muscle fibers with central nuclei were performed with ImageJ. The genotype and sex of the samples were blinded to the analyst.

RNA isolation and qPCR

Flash frozen TA samples were homogenized in Trizol (Life Technologies, Carlsbad, CA) and RNA was isolated from homogenates and treated with Dnase with the Bio-Rad Aurum RNA Isolation Kit (Bio-Rad, Hercules, CA) according to the manufacturer's instructions. RNA was reverse transcribed with iScript™ Reverse Transcription Supermix (Bio-Rad) and qPCR was performed with iTAQ SYBR Green Supermix (Bio-Rad) using 300 nM primers (Table 1), no template controls and no reverse transcriptase controls on a CFX Connect Real Time PCR System (Bio-Rad). Expression values were normalized to glyceraldehyde-3-phosphate dehydrogenase (GAPDH) or Beta-2-Microglobulin (B2M) using the $2^{-\Delta\Delta CT}$ method.

Rotarod Test

Rotarod (Ugo-Basile, Gemonio Italy) tests were performed on post-natal day (P)90 MTg and littermate WT controls and P70, P90, and P110 $SOD1^{G93A}$;MTg and $SOD1^{G93A}$ littermate controls. Acceleration parameters were 5 revolutions per minute (rpm) start speed with an acceleration of 7.2 rpm^2. Three trials were given per day with at least 15 minutes of rest time between trials. To train mice on the rotarod, 2 consecutive days of rotarod trials were administered before obtaining results on day 3. Results from each biological replicate are reported as the average latency to fall time for the 3 trials administered on day 3. Latency to fall was defined as the total amount of time spent on the rotarod, following commencement of acceleration, before the mouse lost its footing causing it to either slip or fall from the rotarod. $SOD1^{G93A}$;MTg and $SOD1^{G93A}$ mice that participated in rotarod trials at multiple ages only underwent training at the youngest age tested.

Four Limb Hanging Test

Hanging tests [30] were performed on p90 MTg and littermate WT controls and p70, p90, and p110 $SOD1^{G93A}$;MTg and $SOD1^{G93A}$ littermates. Mice were weighed before being placed on an aluminum mesh screen composed of 1×1 cm squares. The screen was inverted, placed 40 cm above a padded surface, and observed for a maximum of 600 seconds. Hanging time is defined as the length of time that the mouse maintained its grip on the mesh screen after inversion. Mice that did not fall within 600 seconds of screen inversion were removed from the screen and received the maximum score of 600 seconds. The maximum 600 second score was not achieved by any of the $SOD1^{G93A}$;MTg or $SOD1^{G93A}$ mice. Each mouse underwent 3 trials, separated by 15 minute rest periods, and the best of 3 trials was reported. Mice that refused to participate, by immediately jumping from the screen, were excluded from the study. Results are reported as holding impulse, which is defined as the maximum hang time multiplied by the mouse body weight.

Survival Study

$SOD1^{G93A}$;MTg and $SOD1^{G93A}$ littermates were closely monitored for loss of motor function following symptom onset. Age of survival was defined as the age at which the

animal reached the Virginia Tech IACUC humane endpoint criterion, defined as a righting reflex greater than or equal to 20 seconds.

Statistics

Comparisons between 2 means were made with an unpaired Student's *t*-test or Welch's unpaired Student's *t*-test based on an F-test of variance. For analysis of experiments with 2 variables, comparisons between means were made with a 2-Way ANOVA and Bonferroni post-hoc analysis. A Kolmogorov-Smirnov Test was used to compare the distribution of muscle fiber sizes. A log-rank test was used to evaluate animal survival. An n was defined as one animal for all experiments except comparisons of muscle fiber size distribution (Fig. 2 I, J & Fig. 3 I, J) where an n was defined as one muscle fiber. The Microsoft Excel Data Analysis plugin (RRID:SCR_016137) and GraphPad Prism (RRID: SCR_002798) were used for statistical analyses. Data are expressed as mean ± standard deviation.

Results

Molecular analysis of SOD1^{G93A};MTg skeletal muscle

Previous studies have examined the impact of DMD [22] and SMA [24] on KLF15 expression in skeletal muscles, however, KLF15 expression in ALS-afflicted skeletal muscles is currently unknown. We analyzed KLF15 mRNA levels by qPCR and found that it is not differentially expressed in the TA muscles of pre-symptomatic (P70) or early symptomatic (P90) SOD1^{G93A} mice, as compared to WT littermate controls (Fig. 1 A). To determine whether increasing KLF15 expression improves the health of ALS-afflicted muscles, we crossed the SOD1^{G93A} mouse line with a skeletal muscle-specific KLF15 transgenic line (MTg) [22] to create SOD1^{G93A};MTg mice. In MTg mice, skeletal muscle-specific KLF15 overexpression is driven by the muscle creatine kinase promoter. KLF15 overexpression was confirmed in P90 MTg (Fig. 1B) and SOD1^{G93A};MTg (Fig. 1 C) TA muscles using qPCR. Our qPCR analysis confirmed that KLF15 expression was elevated 4-fold and 3-fold in the TA muscle of healthy adult MTg mice and SOD1^{G93A};MTg mice, respectively, as compared to non-transgenic littermates.

KLF15 overexpression does not protect skeletal muscle from ALS

We assessed the effect of muscle-specific KLF15 overexpression on skeletal muscles afflicted with ALS. We examined the morphology of muscles with varying resistance to ALS-induced pathogenesis in male and female P90 SOD1^{G93A} mice. Disease pathology, including muscle fiber atrophy and NMJ degeneration, is prevalent in hindlimb muscles of SOD1^{G93A} mice at this age [31], however pathology is more severe in the TA as compared to the soleus, which is resistant to ALS [32,33]. Moreover, ALS pathology progresses more rapidly in male, versus female, SOD1^{G93A} mice, regardless of muscle type. Muscle fiber size was evaluated by measuring the minimum Feret's diameter (MFD) of muscle fiber cross sections following delineation of the perimeter of muscle fibers by immunostaining for pan-laminin. In the soleus of healthy control mice, muscle fiber sizes were minimally impacted by muscle overexpression of KLF15 (Fig. 2 A, B, E, F, I, J); where a very modest but statistically significant shift in muscle fiber size distribution was observed in females (Fig. 2 I) but not males (Fig. 2 J). The soleus of SOD1^{G93A} mice was also minimally

impacted by muscle overexpression of KLF15, where a small but statistically significant shift in muscle fiber size distribution was observed in males (Fig. 2 J). In addition, we found no changes in muscle mass associated with muscle KLF15 overexpression in healthy or SOD1^{G93A} mice (Fig. 2 L). Surprisingly, soleus muscle mass was significantly lower in female SOD1^{G93A} mice, regardless of KLF15 overexpression, but not males (Fig. 2 L). Regenerating muscle fibers, as indicated by the presence of a nucleus at the center of the muscle fiber cross section, were infrequently observed in the soleus and were not impacted by genotype (Fig. 2 M).

In the TA, which is more susceptible to ALS, we found that muscle KLF15 overexpression increases the overall distribution of muscle fiber sizes in healthy control mice (Fig. 3 A, B, E, F), with a more robust impact in females (Fig. 3 I) than males (Fig. 3 J). In P90 SOD1^{G93A} mice, muscle overexpression of KLF15 decreased the distribution of muscle fiber sizes in females (Fig. 3 C, D, I) but increased it in males (Fig. 3 G, H, J). These trends were reflected in mean muscle fiber size (Fig. 3 K). Differences in TA muscle mass were not observed in healthy or SOD1^{G93A};MTg mice, as compared to littermate controls, however TA muscle mass was lower in male and female SOD1^{G93A} mice, regardless of KLF15 overexpression (Fig. 3 L). As in the soleus, significant differences in regenerating muscle fibers related to muscle KLF15 overexpression were not observed in healthy or SOD1^{G93A} TA muscles (Fig. 3 M).

Overexpressing KLF15 in muscles does not affect the structure of the NMJ postsynapse

Declining health of ALS-afflicted muscles is associated with degeneration of NMJ endplates, characterized by fragmentation of nicotinic acetylcholine receptors (AChRs) clusters and decreased endplate area [27]. To evaluate the impact of muscle-specific KLF15 overexpression on NMJ integrity, we visualized NMJs in the EDL muscle following labeling of AChRs with fluorescently conjugated alpha-bungarotoxin (fBTX) (Fig. 4 A–H). We did not observe differences associated with muscle KLF15 overexpression in the overall area (Fig. 4 I) or fragmentation (Fig. 4 J) of postsynaptic AChRs in P90 healthy control or SOD1^{G93A} mice. Together, these results suggest that increased expression of KLF15 in skeletal muscles has no discernible impact on muscle fiber atrophy during the early symptomatic stages in SOD1^{G93A} mice or NMJ endplate morphology in healthy or SOD1^{G93A} mice.

Muscle-specific KLF15 overexpression does not slow ALS-pathogenesis in mice

We next asked whether muscle-specific KLF15 overexpression impacts body weight, motor function, or muscle strength in SOD1^{G93A} mice. Similar body weights were observed in MTg versus non-transgenic controls in both the SOD1^{G93A} and healthy cohorts (Fig. 5 A–C). Analysis of motor function using the rotarod test in healthy adult (P90) WT and MTg littermates showed that the average latency to fall time is not impacted by muscle-specific KLF15 overexpression (Fig. 5 D). Analysis of pre-symptomatic (p70), early symptomatic (p90), and symptomatic (p110) SOD1^{G93A} and SOD1^{G93A};MTg littermates showed a progressive age-related decrease in rotarod performance, regardless of genotype, in females (Fig. 5 E), and males (Fig. 5 F), however, rotarod performance was not impacted by muscle overexpression of KLF15. Evaluation of muscle strength using the four-limb

hanging test showed no differences related to muscle KLF15 overexpression in healthy control (Fig. 5 G) or SOD1^{G93A} (Fig. 5 H, I) mice, however an age-related loss of muscle strength was observed in males and females, regardless of genotype (Fig. 5 H, I). These results suggest that muscle KLF15 overexpression does not impact the onset or progression of motor function loss in SOD1^{G93A} mice.

Muscle-specific KLF15 overexpression does not extend survival of SOD1^{G93A} mice

A survival analysis was performed to determine if muscle-specific KLF15 overexpression has a global, long-term impact on ALS disease progression in SOD1^{G93A} mice. Differences in lifespan were not observed in male or female SOD1^{G93A};MTg mice when compared to sex-matched SOD1^{G93A} littermate controls (Fig. 6). The mean survival ages for SOD1^{G93A} and SOD1^{G93A};MTg mice, respectively, were 157.7 ± 12.4 d and 155.6 ± 10.0 d for females (Fig. 6 A), and 145.2 ± 11.4 d and 150.3 ± 11.0 d for males (Fig. 6 C), and 151.1 ± 13.2 d and 152.2 d ± 10.8 d for males and females combined (Fig. 6 E).

These results provide further evidence that disease progression and ALS pathology in SOD1^{G93A} mice are not impacted by muscle KLF15 overexpression.

KLF15 overexpression fails to induce expression of protective genes in SOD1^{G93A} mice

The absence of improvement in skeletal muscle health in SOD1^{G93A};MTg mice led us to ask whether KLF15 overexpression affected the expression of genes with important roles in the health of NMJs and muscle fibers. Previous transcriptomic analysis of the quadriceps muscle from healthy adult MTg mice demonstrated that KLF15 promotes the expression of *Fgfbp1* [22], a gene which has been shown to play a protective role in ALS-afflicted skeletal muscles [26]. Our qPCR analysis of the TA muscle showed that while FGFBP1 is elevated 2-fold in healthy adult MTg mice, as compared to WT littermates (Fig. 7 A), it is not elevated in SOD1^{G93A};MTg versus SOD1^{G93A} littermates (Fig. 7 B). We also failed to see a change in the expression of CD36 antigen/fatty acid translocase (CD36) in the TA of SOD1^{G93A};MTg mice (Fig. 7 C). This gene is regulated by KLF15, promotes lipid metabolism [23] and is upregulated in the TA muscles of early symptomatic SOD1^{G86R} mice [15]. Further analysis of markers for metabolic substrate availability and muscle atrophy in TA muscles, including peroxisome proliferator-activated receptor-gamma coactivator-1α (PGC1α), tripartite motif containing 63 (TRIM63), eukaryotic translation initiation factor 4E (EIF4E) and EIF4E binding protein 1 (EIF4EBP1) [34], revealed no differences in transcript levels between SOD1^{G93A} and SOD1^{G93A};MTg littermates (Fig. 7 D–G). These results provide evidence that KLF15 overexpression in SOD1^{G93A} muscle has little impact on the transcription of genes in key metabolic and atrophy signaling pathways. These data also suggest that upstream inhibitors of KLF15 block its ability to promote transcription of target genes in ALS.

Discussion

KLF15 is a key regulator of metabolic plasticity in skeletal muscle during physiological and disease-related stress [20,21]. Increased energy expenditure and utilization of alternative energy sources such as amino acids and fatty acids by skeletal muscles are hallmarks of

ALS and are thought to contribute to progressive muscle atrophy and motor degeneration associated with the disease [18]. We asked whether overexpression of KLF15 by skeletal muscles could prevent muscle atrophy, NMJ postsynaptic degeneration, and loss of motor function in the $SOD1^{G93A}$ mouse model of ALS. Our analysis of hindlimb skeletal muscles with varying fiber type composition and disease susceptibility showed that muscle-specific KLF15 overexpression had a negligible impact on the health of the soleus (Fig. 2) and TA (Fig. 3) muscles of early symptomatic ALS mice. These results were supported by rotarod and four-limb hanging tests which showed a similar lack of improvement in motor function in symptomatic muscle-specific KLF15 overexpressing $SOD1^{G93A}$ mice (Fig. 5). Moreover, mean survival time of $SOD1^{G93A}$ mice was not impacted by muscle-specific KLF15 overexpression (Fig. 6). Unexpectedly, KLF15 overexpression did not impact transcript levels of genes with known roles in the health of ALS-afflicted muscles that are under direct regulatory control of KLF15, including FGFBP1[22] and CD36 [23]. Taken together, the results of this study show that chronically increasing KLF15 expression in skeletal muscle at a level of approximately 3-fold over baseline does not improve disease outcome in the $SOD1^{G93A}$ ALS mouse model.

Our findings are surprising in light of previous studies showing that transgenic KLF15 overexpression improves the health of chronically stressed muscles in mouse models of DMD [22] and SMA [24]. KLF15 has recently been directly implicated in supporting muscle mitochondrial function, in addition to activating alternative metabolic pathways, by promoting several genes of the mitochondrial carnitine shuttle [23]. In this capacity, KLF15 increases mitochondrial access to long chain fatty acids [23] which are an increasingly important energy substrate for muscle mitochondria in the symptomatic stages of ALS [18]. Indeed, efforts to boost mitochondrial carnitine shuttling have extended survival of $SOD1^{G93A}$ mice [35], although they have shown limited success in ALS patients [36]. Our observation that CD36, a protein that promotes fatty acid metabolism and is regulated by KLF15 [23], is not upregulated in $SOD1^{G93A}$;MTg muscle suggests that the lack of a rescue phenotype in $SOD1^{G93A}$;MTg mice may be due in part to a disruption in KLF15-mediated activation of key alternative metabolic pathways by $SOD1^{G93A}$ pathology. It is also possible that, despite the efforts of KLF15 to activate alternate metabolic pathways in energetically deprived skeletal muscles, severely dysfunctional mitochondria are simply unable to utilize these alternative energy sources. Indeed, impairment of mitochondrial function has been well documented in skeletal muscles of ALS models and patients [10–13].

A second explanation for the absence of a distinct phenotype in $SOD1^{G93A}$;MTg mice is that the availability of alternate energy substrates, rather than KLF15, may be the rate-limiting factor in meeting the increased energy demands of ALS-afflicted muscle. Previous studies have demonstrated that energy substrate scarcity is a hallmark of ALS. Hypolipidemia is common in male ALS patients [37] and $SOD1^{G93A}$ mice [38,39] and obesity is a negative ALS risk factor [40]. Efforts to delay ALS progression through implementation of high energy diets have been successful in $SOD1^{G93A}$ mice [14] but have had mixed success in ALS patients [41]. Therefore, it is possible that alternate energy sources, such as lipid stores, are depleted in presymptomatic $SOD1^{G93A}$ mice, a process that may even be accelerated by increased KLF15 levels, obviating any benefits related to KLF15 overexpression.

Experimental conditions may also factor into our failure to observe a clear phenotype in muscle KLF15 overexpressing SOD1^{G93A} mice. For example, it is possible that KLF15 was not sufficiently induced to alter ALS pathology at the timepoints observed in our study. We observed an approximately four-fold increase in KLF15 mRNA expression in healthy MTg TA muscle (Fig. 1B), however this increase was slightly diminished in SOD1^{G93A};MTg muscle (Fig. 1 C). This increase is somewhat less robust than that of previous studies of MTg mice [22,24], which may reflect differences related to the SOD1^{G93A} allele or the background of this strain. In a recent study, SMA pathology was not improved following adeno-associated virus-mediated (AAV) KLF15 overexpression [25]. The authors of this study propose that differences in the extent to which KLF15 is overexpressed may impact its therapeutic potential, noting previous studies that demonstrate that changes in KLF15 abundance impact expression of atrophy versus ergogenic genes. Timing may have been another factor. Our observations of muscle fiber atrophy were limited to a single timepoint (P90). While few previous studies have examined the timing of muscle atrophy in the SOD1^{G93A} model, particularly at a histological level, there is clear evidence of pronounced atrophy of predominately fast-twitch skeletal muscles as early as 60 days of age in SOD1^{G93A} mice [32,33]. Therefore, KLF15 overexpression may have a significant impact on muscle fiber atrophy during earlier disease stages, or perhaps even end stages, which were not observed in this study. Nonetheless, we did not detect appreciable differences in motor function or survival in SOD1^{G93A};MTg mice.

An intriguing finding in our study is that muscle mass is lost in both the TA and soleus of female SOD1^{G93A} mice without a concomitant decrease in muscle fiber size at 90 days of age. This pattern of muscle atrophy was not evident in SOD1^{G93A} males, where decreases in both muscle mass and muscle fiber size were observed in the TA but not the soleus (Fig. 2 & 3). These results suggest that muscle fiber loss, rather than reductions in muscle fiber size, may be a major driver of pathology in female SOD1^{G93A} mice. While muscle fiber atrophy has been evaluated in the TA of SOD1^{G93A} mice [32,33], to our knowledge sex-related differences in this process have not been reported, and hence they are an area of interest for future studies. More relevant to the current study, our data suggest that negative regulators of KLF15 are prevalent, active and prevent KLF15 from increasing expression of genes important for NMJ and muscle health in ALS. Thus, future studies should focus on discovering and targeting such negative regulators of KLF15 rather than increasing KLF15 expression to preserve the health of NMJs and muscles in ALS.

Acknowledgements

This work was funded through grants from the National Institute on Aging (R01AG055545 and R56AG051501) and the National Institute of Neurological Disorders and Stroke (R21NS106313) awarded to GV.

We would like to thank members of the Valdez laboratory for assistance in editing the manuscript. A special thanks to B. Drummond and J. Cauty for providing inspiration for this project.

References

[1]. Kim G, Gautier O, Tassoni-Tsuchida E, Ma XR, Gitler AD, ALS Genetics: Gains, Losses, and Implications for Future Therapies, Neuron. 108 (2020) 822–842. doi:10.1016/j.neuron.2020.08.022. [PubMed: 32931756]

[2]. Loeffler JP, Picchiarelli G, Dupuis L, Gonzalez De Aguilar JL, The role of skeletal muscle in amyotrophic lateral sclerosis, in: Brain Pathol, Blackwell Publishing Ltd, 2016: pp. 227–236. doi:10.1111/bpa.12350.

[3]. Moloney EB, de Winter F, Verhaagen J, ALS as a distal axonopathy: molecular mechanisms affecting neuromuscular junction stability in the presymptomatic stages of the disease., Front. Neurosci. 8 (2014) 252. doi:10.3389/fnins.2014.00252. [PubMed: 25177267]

[4]. Killian JM, Wilfong AA, Burnett L, Appel SH, Boland D, Decremental motor responses to repetitive nerve stimulation in ALS, Muscle Nerve. 17 (1994) 747–754. doi:10.1002/mus.880170708. [PubMed: 8008001]

[5]. Fischer LR, Culver DG, Tennant P, Davis AA, Wang M, Castellano-Sanchez A, Khan J, Polak MA, Glass JD, Amyotrophic lateral sclerosis is a distal axonopathy: evidence in mice and man, Exp. Neurol. 185 (2004) 232–240. doi:10.1016/J.EXPNEUROL.2003.10.004. [PubMed: 14736504]

[6]. Pun S, Santos AF, Saxena S, Xu L, Caroni P, Selective vulnerability and pruning of phasic motoneuron axons in motoneuron disease alleviated by CNTF, Nat. Neurosci. 9 (2006) 408–419. doi:10.1038/nn1653. [PubMed: 16474388]

[7]. Dobrowolny G, Aucello M, Rizzuto E, Beccafico S, Mammucari C, Boncompagni S, Belia S, Wannenes F, Nicoletti C, Del Prete Z, Rosenthal N, Molinaro M, Protasi F, Fanò G, Sandri M, Musarò A, Skeletal Muscle Is a Primary Target of SOD1G93A-Mediated Toxicity, Cell Metab. 8 (2008) 425–436. doi:10.1016/j.cmet.2008.09.002. [PubMed: 19046573]

[8]. Wong M, Martin LJ, Skeletal muscle-restricted expression of human SOD1 causes motor neuron degeneration in transgenic mice, Hum. Mol. Genet. 19 (2010) 2284–2302. doi:10.1093/hmg/ddq106. [PubMed: 20223753]

[9]. Martin LJ, Wong M, Skeletal Muscle-Restricted Expression of Human SOD1 in Transgenic Mice Causes a Fatal ALS-Like Syndrome, Front. Neurol. 11 (2020). doi:10.3389/fneur.2020.592851.

[10]. Myoung JC, Suh YL, Ultrastructural changes of mitochondria in the skeletal muscle of patients with amyotrophic lateral sclerosis, Ultrastruct. Pathol. 26 (2002) 3–7. doi:10.1080/01913120252934260. [PubMed: 12028652]

[11]. Echaniz-Laguna A, Zoll J, Ponsot E, N'Guessan B, Tranchant C, Loeffler JP, Lampert E, Muscular mitochondrial function in amyotrophic lateral sclerosis is progressively altered as the disease develops: A temporal study in man, Exp. Neurol. 198 (2006) 25–30. doi:10.1016/j.expneurol.2005.07.020. [PubMed: 16126198]

[12]. Krasnianski A, Deschauer M, Neudecker S, Gellerich FN, Müller T, Schoser BG, Krasnianski M, Zierz S, Mitochondrial changes in skeletal muscle in amyotrophic lateral sclerosis and other neurogenic atrophies, Brain. 128 (2005) 1870–1876. doi:10.1093/brain/awh540. [PubMed: 15901649]

[13]. Vielhaber S, Winkler K, Kirches E, Kunz D, Büchner M, Feistner H, Elger CE, Ludolph AC, Riepe MW, Kunz WS, Visualization of defective mitochondrial function in skeletal muscle fibers of patients with sporadic amyotrophic lateral sclerosis, J. Neurol. Sci. 169 (1999) 133–139. doi:10.1016/S0022-510X(99)00236-1. [PubMed: 10540022]

[14]. Dupuis L, Oudart H, René F, Gonzalez De Aguilar JL, Loeffler JP, Evidence for defective energy homeostasis in amyotrophic lateral sclerosis: Benefit of a high-energy diet in a transgenic mouse model, Proc. Natl. Acad. Sci. U. S. A. 101 (2004) 11159–11164. doi:10.1073/pnas.0402026101. [PubMed: 15263088]

[15]. Palamiuc L, Schlagowski A, Ngo ST, Vernay A, Dirrig-Grosch S, Henriques A, Boutillier A, Zoll J, Echaniz-Laguna A, Loeffler J, René F, A metabolic switch toward lipid use in glycolytic muscle is an early pathologic event in a mouse model of amyotrophic lateral sclerosis, EMBO Mol. Med. 7 (2015) 526–546. doi:10.15252/emmm.201404433. [PubMed: 25820275]

[16]. Steyn FJ, Li R, Kirk SE, Tefera TW, Xie TY, Tracey TJ, Kelk D, Wimberger E, Garton FC, Roberts L, Chapman SE, Coombes JS, Leevy WM, Ferri A, Valle C, René F, Loeffler J-P, McCombe PA, Henderson RD, Ngo ST, Altered skeletal muscle glucose-fatty acid flux in amyotrophic lateral sclerosis, Brain Commun. 2 (2020). doi:10.1093/braincomms/fcaa154.

[17]. Dobrowolny G, Lepore E, Martini M, Barberi L, Nunn A, Scicchitano BM, Musarò A, Metabolic changes associated with muscle expression of SOD1G93A, Front. Physiol. 9 (2018). doi:10.3389/fphys.2018.00831.

[18]. Vandoorne T, De Bock K, Van Den Bosch L, Energy metabolism in ALS: an underappreciated opportunity?, Acta Neuropathol. 135 (2018) 489–509. doi:10.1007/s00401-018-1835-x. [PubMed: 29549424]

[19]. Argilés JM, Campos N, Lopez-Pedrosa JM, Rueda R, Rodriguez-Mañas L, Skeletal Muscle Regulates Metabolism via Interorgan Crosstalk: Roles in Health and Disease, J. Am. Med. Dir. Assoc. 17 (2016) 789–796. doi:10.1016/j.jamda.2016.04.019. [PubMed: 27324808]

[20]. Haldar SM, Jeyaraj D, Anand P, Zhu H, Lu Y, Prosdocimo DA, Eapen B, Kawanami D, Okutsu M, Brotto L, Fujioka H, Kerner J, Rosca MG, McGuinness OP, Snow RJ, Russell AP, Gerber AN, Bai X, Yan Z, Nosek TM, Brotto M, Hoppel CL, Jain MK, Kruppel-like factor 15 regulates skeletal muscle lipid flux and exercise adaptation, Proc. Natl. Acad. Sci. U. S. A. 109 (2012) 6739–6744. doi:10.1073/pnas.1121060109. [PubMed: 22493257]

[21]. Haldar SM, Ibrahim OA, Jain MK, Kruppel-like Factors (KLFs) in muscle biology, J. Mol. Cell. Cardiol. 43 (2007) 1–10. doi:10.1016/j.yjmcc.2007.04.005. [PubMed: 17531262]

[22]. Morrison-Nozik A, Anand P, Zhu H, Duan Q, Sabeh M, Prosdocimo DA, Lemieux ME, Nordsborg N, Russell AP, MacRae CA, Gerber AN, Jain MK, Haldar SM, Glucocorticoids enhance muscle endurance and ameliorate Duchenne muscular dystrophy through a defined metabolic program., Proc. Natl. Acad. Sci. U. S. A. 112 (2015) E6780–9. doi:10.1073/pnas.1512968112. [PubMed: 26598680]

[23]. Fan L, Sweet DR, Prosdocimo DA, Vinayachandran V, Chan ER, Zhang R, Ilkayeva O, Lu Y, Keerthy KS, Booth CE, Newgard CB, Jain MK, Muscle Krüppel-like factor 15 regulates lipid flux and systemic metabolic homeostasis, J. Clin. Invest. 131 (2021). doi:10.1172/JCI139496.

[24]. Walter LM, Deguise MO, Meijboom KE, Betts CA, Ahlskog N, van Westering TLE, Hazell G, McFall E, Kordala A, Hammond SM, Abendroth F, Murray LM, Shorrock HK, Prosdocimo DA, Haldar SM, Jain MK, Gillingwater TH, Claus P, Kothary R, Wood MJA, Bowerman M, Interventions Targeting Glucocorticoid-Krüppel-like Factor 15-Branched-Chain Amino Acid Signaling Improve Disease Phenotypes in Spinal Muscular Atrophy Mice, EBioMedicine. 31 (2018) 226–242. doi:10.1016/j.ebiom.2018.04.024. [PubMed: 29735415]

[25]. Ahlskog N, Hayler D, Krueger A, Kubinski S, Claus P, Hammond SM, Wood MJA, Yáñez-Muñoz RJ, Bowerman M, Muscle overexpression of Klf15 via an AAV8-Spc5-12 construct does not provide benefits in spinal muscular atrophy mice, Gene Ther. 27 (2020) 505–515. doi:10.1038/s41434-020-0146-8.

[26]. Taetzsch T, Tenga MJ, Valdez G, Muscle Fibers Secrete FGFBP1 to Slow Degeneration of Neuromuscular Synapses during Aging and Progression of ALS., J. Neurosci. 37 (2017) 70–82. doi:10.1523/JNEUROSCI.2992-16.2017. [PubMed: 28053031]

[27]. Valdez G, Tapia JC, Lichtman JW, Fox MA, Sanes JR, Shared resistance to aging and ALS in neuromuscular junctions of specific muscles., PLoS One. 7 (2012) e34640. doi:10.1371/journal.pone.0034640. [PubMed: 22485182]

[28]. Gurney ME, Pu H, Chiu AY, Dal Canto MC, Polchow CY, Alexander DD, Caliendo J, Hentati A, Kwon YW, Deng HX, Motor neuron degeneration in mice that express a human Cu,Zn superoxide dismutase mutation., Science. 264 (1994) 1772–5. http://www.ncbi.nlm.nih.gov/pubmed/8209258 (accessed December 9, 2014). [PubMed: 8209258]

[29]. Mouton PR, Unbiased stereology : a concise guide/, Johns Hopkins University Press, Baltimore :, 2011.

[30]. Aartsma-Rus A, van Putten M, Assessing functional performance in the Mdx mouse model, J. Vis. Exp. 85 (2014) 51303. doi:10.3791/51303.

[31]. Marcuzzo S, Zucca I, Mastropietro A, de Rosbo NK, Cavalcante P, Tartari S, Bonanno S, Preite L, Mantegazza R, Bernasconi P, Hind limb muscle atrophy precedes cerebral neuronal degeneration in G93A-SOD1 mouse model of amyotrophic lateral sclerosis: A longitudinal MRI study, Exp. Neurol. 231 (2011) 30–37. doi:10.1016/j.expneurol.2011.05.007. [PubMed: 21620832]

[32]. Hegedus J, Putman CT, Tyreman N, Gordon T, Preferential motor unit loss in the SOD1 G93A transgenic mouse model of amyotrophic lateral sclerosis, J. Physiol. 586 (2008) 3337–3351. doi:10.1113/jphysiol.2007.149286. [PubMed: 18467368]

[33]. Hegedus J, Putman CT, Gordon T, Time course of preferential motor unit loss in the SOD1G93A mouse model of amyotrophic lateral sclerosis, Neurobiol. Dis. 28 (2007) 154–164. doi:10.1016/j.nbd.2007.07.003. [PubMed: 17766128]

[34]. Tintignac LA, Brenner HR, Rüegg MA, Mechanisms regulating neuromuscular junction development and function and causes of muscle wasting, Physiol. Rev. 95 (2015) 809–852. doi:10.1152/physrev.00033.2014. [PubMed: 26109340]

[35]. Kira Y, Nishikawa M, Ochi A, Sato E, Inoue M, L-Carnitine suppresses the onset of neuromuscular degeneration and increases the life span of mice with familial amyotrophic lateral sclerosis, Brain Res. 1070 (2006) 206–214. doi:10.1016/j.brainres.2005.11.052. [PubMed: 16412993]

[36]. Beghi E, Pupillo E, Bonito V, Buzzi P, Caponnetto C, Chiò A, Corbo M, Giannini F, Inghilleri M, La Bella V, Logroscino G, Lorusso L, Lunetta C, Mazzini L, Messina P, Mora G, Perini M, Quadrelli ML, Silani V, Simone IL, Tremolizzo L, Samarelli V, Tortelli R, D'Errico E, Merello M, Tavernelli F, Mancardi GL, Mascolo M, Bendotti C, Buratti M, Floriani I, Giordano L, Giussani G, Maderna L, Maestri E, Marinou K, Mennini T, Messina S, Morelli C, Papetti L, Rizzo A, Ticozzi N, Verde F, Ferrarese C, Marzorati L, Testa L, Valentino F, Frasca V, Giacomelli E, Casa S, Malentacchi M, Calvo A, Cammarosano S, Moglia C, Cavallo E, Fuda G, Randomized double-blind placebo-controlled trial of acetyl-L-carnitine for ALS, Amyotroph. Lateral Scler. Front. Degener. 14 (2013) 397–405. doi:10.3109/21678421.2013.764568.

[37]. Yang JW, Kim S-M, Kim H-J, Kim J-E, Park KS, Kim S-H, Lee K-W, Sung J-J, Hypolipidemia in Patients with Amyotrophic Lateral Sclerosis: A Possible Gender Difference?, J. Clin. Neurol. 9 (2013) 125. doi:10.3988/jcn.2013.9.2.125. [PubMed: 23626651]

[38]. Kim S-M, Kim H, Kim J-E, Park KS, Sung J-J, Kim SH, Lee K-W, Amyotrophic Lateral Sclerosis Is Associated with Hypolipidemia at the Presymptomatic Stage in Mice, PLoS One. 6 (2011) e17985. doi:10.1371/journal.pone.0017985. [PubMed: 21464953]

[39]. Fergani A, Oudart H, De Aguilar JLG, Fricker B, René F, Hocquette JF, Meininger V, Dupuis L, Loeffler JP, Increased peripheral lipid clearance in an animal model of amyotrophic lateral sclerosis, J. Lipid Res. 48 (2007) 1571–1580. doi:10.1194/jlr.M700017-JLR200. [PubMed: 17438338]

[40]. O'Reilly ÉJ, Wang H, Weisskopf MG, Fitzgerald KC, Falcone G, McCullough ML, Thun M, Park Y, Kolonel LN, Ascherio A, Premorbid body mass index and risk of amyotrophic lateral sclerosis, Amyotroph. Lateral Scler. Front. Degener. 14 (2013) 205–211. doi:10.3109/21678421.2012.735240.

[41]. Ludolph AC, Dorst J, Dreyhaupt J, Weishaupt JH, Kassubek J, Weiland U, Meyer T, Petri S, Hermann A, Emmer A, Grosskreutz J, Grehl T, Zeller D, Boentert M, Schrank B, Prudlo J, Winkler AS, Gorbulev S, Roselli F, Schuster J, Dupuis L, Effect of High-Caloric Nutrition on Survival in Amyotrophic Lateral Sclerosis, Ann. Neurol. 87 (2020) 206–216. doi:10.1002/ana.25661. [PubMed: 31849093]

- Muscle-specific KLF15 overexpression did not affect ALS pathology in $SOD1^{G93A}$ mice.
- KLF15 overexpression had no effect on NMJs and muscle fibers in $SOD1^{G93A}$ mice
- KLF15 failed to increase expression of target genes in in $SOD1^{G93A}$ mice.
- In ALS, negative regulators of KLF15 may inhibit its function in skeletal muscles.

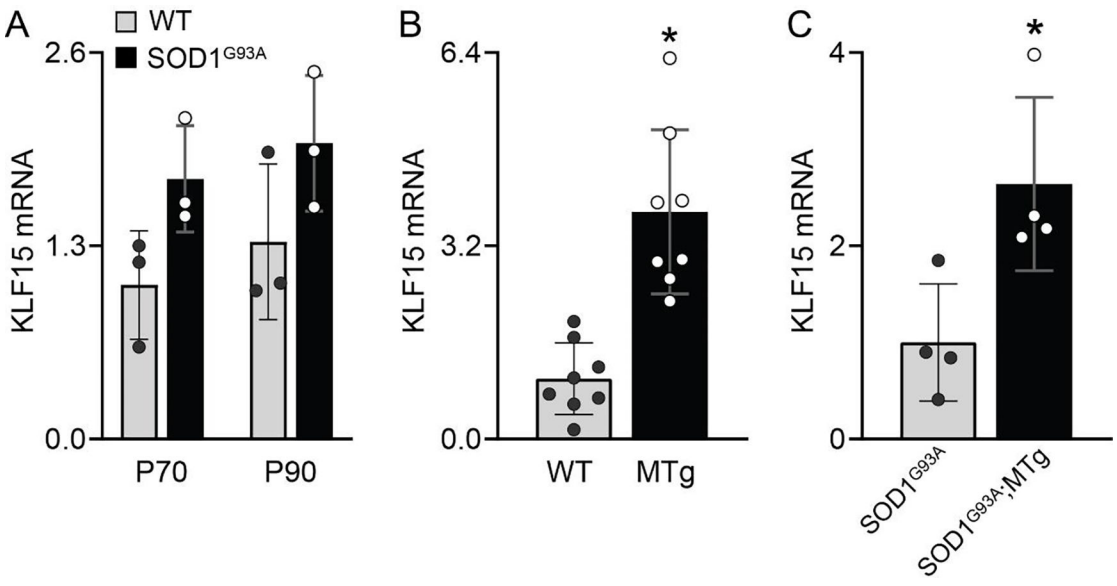

Figure 1.

qPCR analysis of KLF15 mRNA in WT, SOD1^{G93A}, MTg and SOD1^{G93A};MTg TA muscles. (A) P70 and P90 WT and SOD1^{G93A}. (B) P90 WT and MTg. (C) P90 SOD1^{G93A} and SOD1^{G93A};MTg. All values reported as mean ± SD; n = 3 (A), 8 (B), 4 (C). * $p < 0.05$

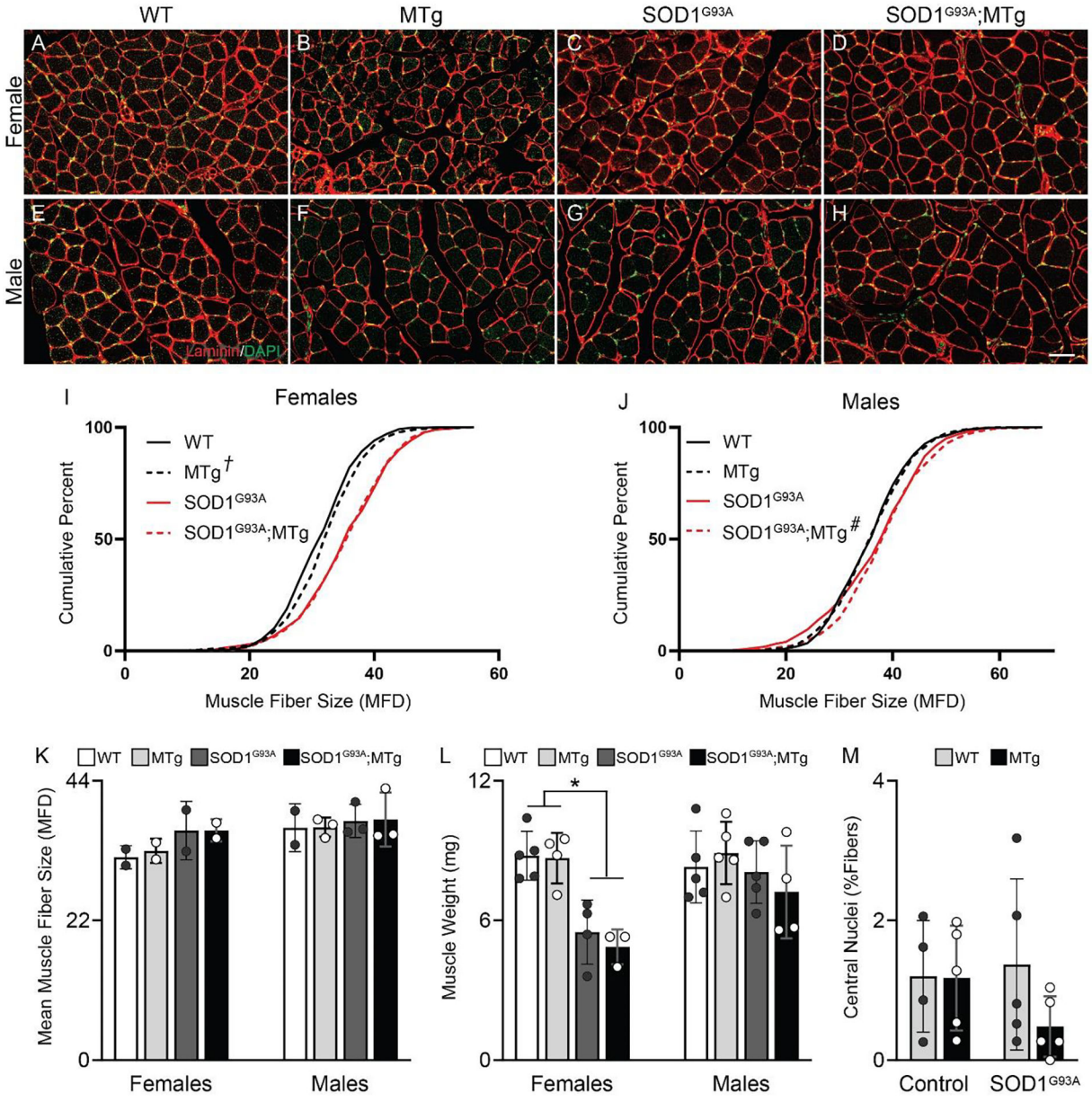

Figure 2.

Assessment of soleus muscle atrophy in P90 MTg SOD1^{G93A} and healthy control mice. (A-H) Representative images of laminin IHC in soleus muscle cross sections of female and male mice. (I,J) Cumulative distribution plots of muscle fiber sizes based on minimum Feret's diameter (MFD) measurements of muscle fiber cross sections. (I) Female mice, n ≥ 736 muscle fibers/genotype. (J) Male mice, n ≥ 739 muscle fibers/genotype. (K) Mean soleus muscle fiber size, n ≥ 2 mice. (L) Mean soleus muscle weight, n ≥ 3 mice. (M) Mean percentage of regenerating muscle fibers, identified by the presence of a centrally located nuclei within the muscle fiber cross section, n ≥ 4 mice. Averages in panel M represent males and females. † $p < 0.05$ versus WT, Kolmogorov-Smirnov Test. # $p < 0.05$ versus SOD1^{G93A}, Kolmogorov-Smirnov Test. * $p < 0.05$, SOD1^{G93A} genotype effect, 2-way ANOVA. Scale bar = 50 μm. Values in panels K-M are mean ± S.D.

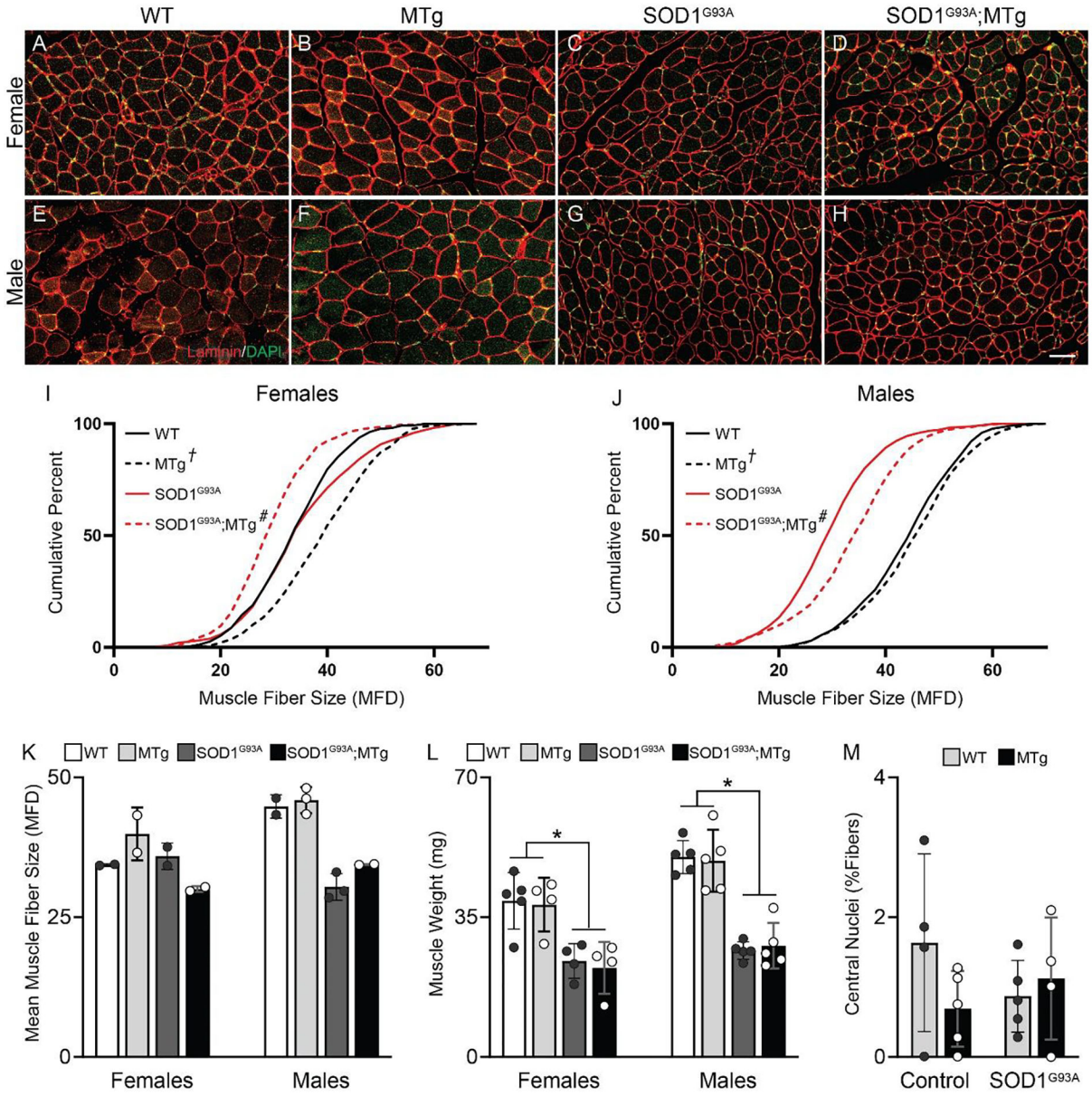

Figure 3.

Assessment of TA muscle atrophy in P90 MTg SOD1^{G93A} and healthy control mice. (A-H) Representative images of laminin IHC in TA muscle cross sections of female and male mice. (I,J) Cumulative distribution plots of muscle fiber sizes based on minimum Feret's diameter (MFD) measurements of muscle fiber cross sections. (I) Female mice, n ≥ 717 muscle fibers/genotype. (J) Male mice, n ≥ 738 muscle fibers/genotype. (K) Mean TA muscle fiber size, n ≥ 2 mice. (L) Mean TA muscle weight, n ≥ 4 mice. (M) Mean percentage of regenerating muscle fibers, identified by the presence of a centrally located nuclei within the muscle fiber cross section, n ≥ 4 mice. Averages in panel M represent males and females. † $p < 0.05$ versus WT, Kolmogorov-Smirnov Test. # $p < 0.05$ versus SOD1^{G93A}, Kolmogorov-Smirnov Test. * $p < 0.05$, SOD1^{G93A} genotype effect, 2-way ANOVA. Scale bar = 50 μm. Values in panels K-M are mean ± S.D.

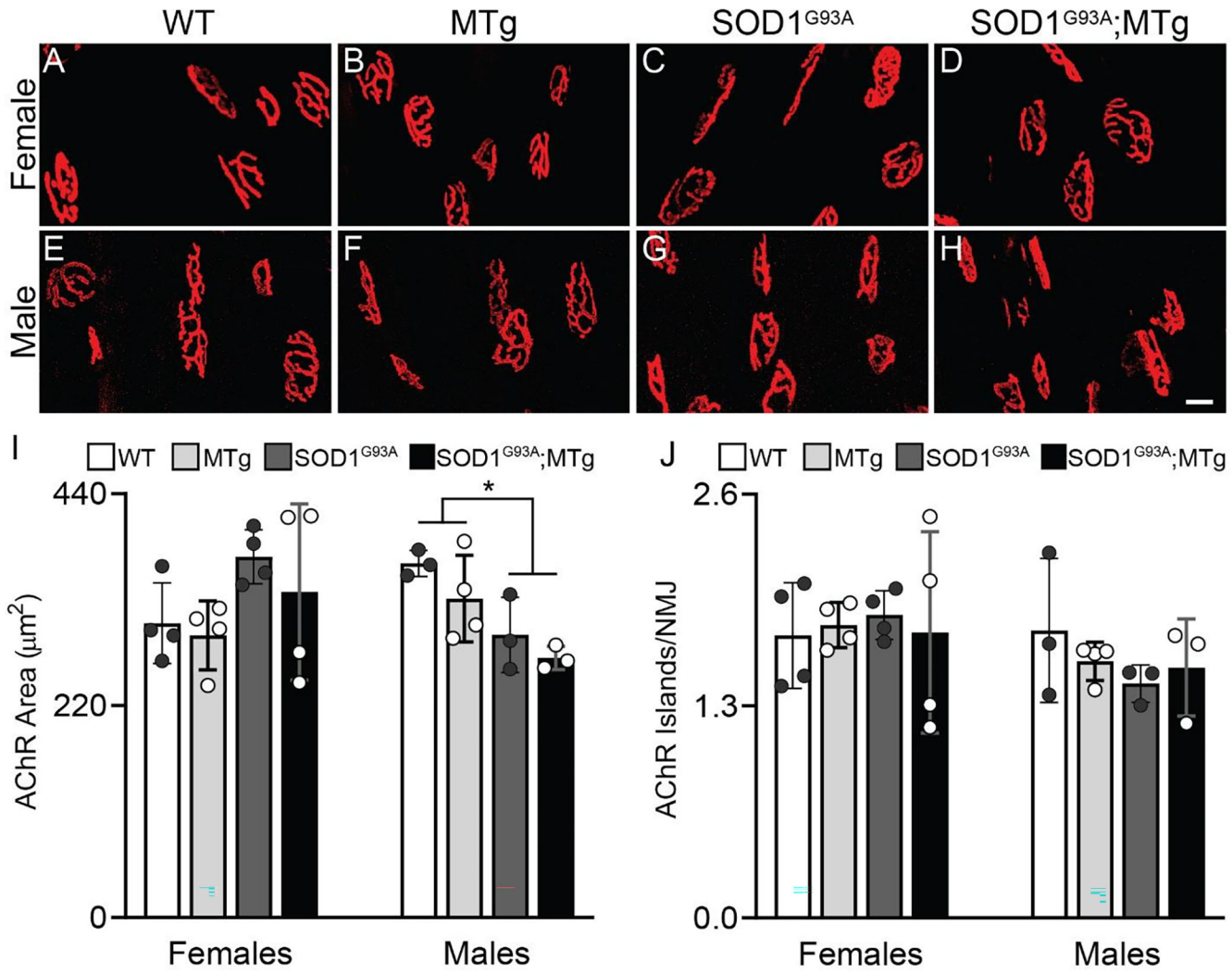

Figure 4.

Assessment of NMJ postsynaptic integrity in P90 MTg SOD1^{G93A} and healthy control mice. (A-H) Representative images of AChRs of the NMJ post-synapse labeled with fBTX. (I) Mean area of fBTX-labeled AChR postsynaptic area. (J) Fragmentation of AChR clusters, determined by the mean number of discrete AChR islands per NMJ. * $p < 0.05$, SOD1^{G93A} genotype effect, 2-way ANOVA. N = 3–4. Scale bar = 20 μm. Values are mean ± S.D.

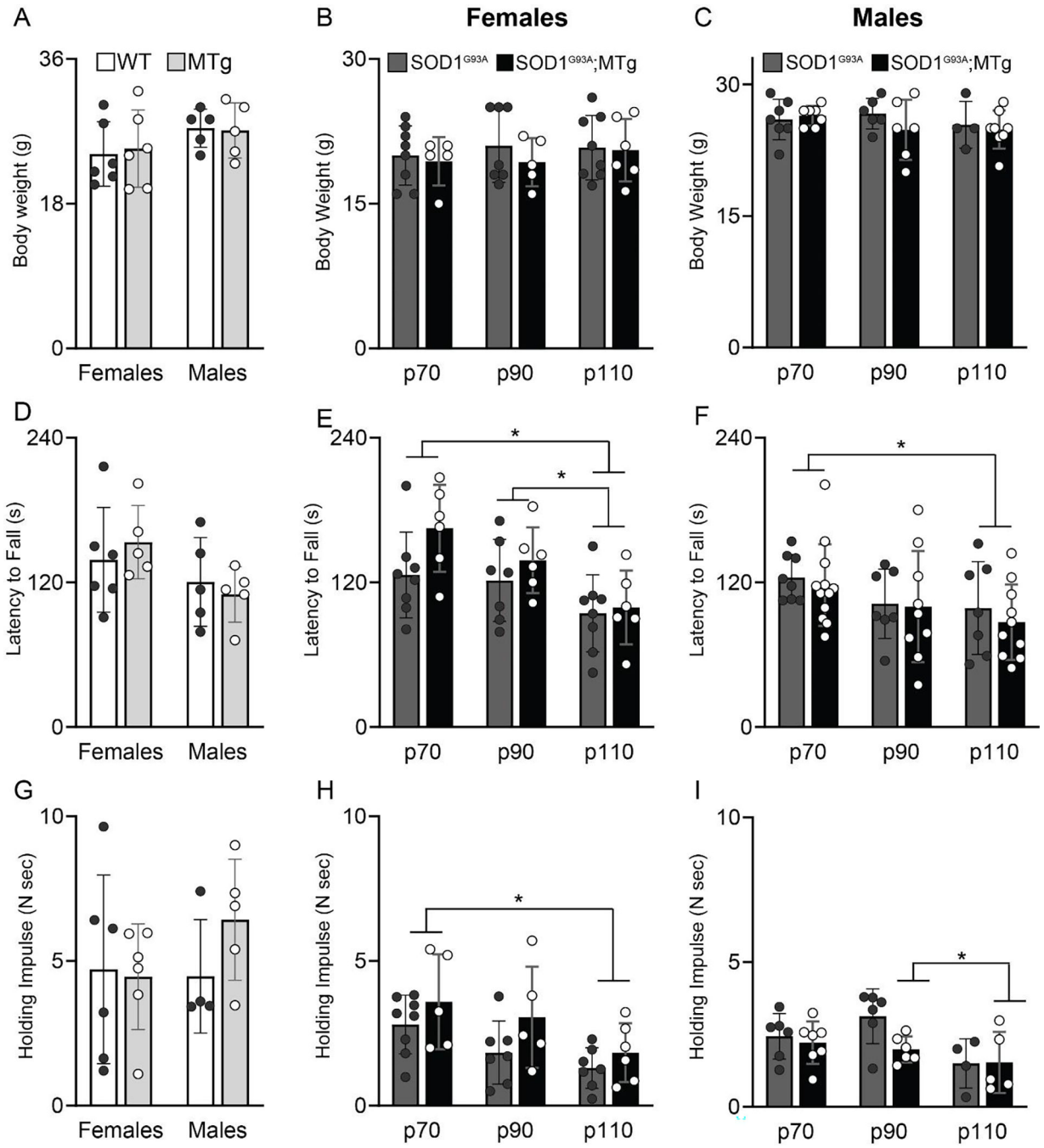

Figure 5.

Body weight and motor function are not altered in MTg SOD1^{G93A} or healthy control mice. (A-C) Mouse body weight comparisons. (A) P90 healthy control WT versus MTg. n = 5–6. (B) Female SOD1^{G93A} versus SOD1^{G93A};MTg. n = 5–8. (C) Male SOD1^{G93A} versus SOD1^{G93A};MTg. n = 4–8. (D-F) Average rotarod test latency to fall times. (D) P90 healthy control WT versus MTg. n = 5–6. (E) Female SOD1^{G93A} versus SOD1^{G93A};MTg. n = 6–8. (F) Male SOD1^{G93A} versus SOD1^{G93A};MTg. n = 7–11. (G-I) Average holding impulse scores in the four limb hanging test. (G) P90 healthy control WT versus MTg. n =

4–6. (H) Female SOD1^{G93A} versus SOD1^{G93A};MTg. n = 4–7. (I) Male SOD1^{G93A} versus SOD1^{G93A};MTg. n = 4–7. Values are mean ± S.D. * $p < 0.05$ age effect, 2-way ANOVA.

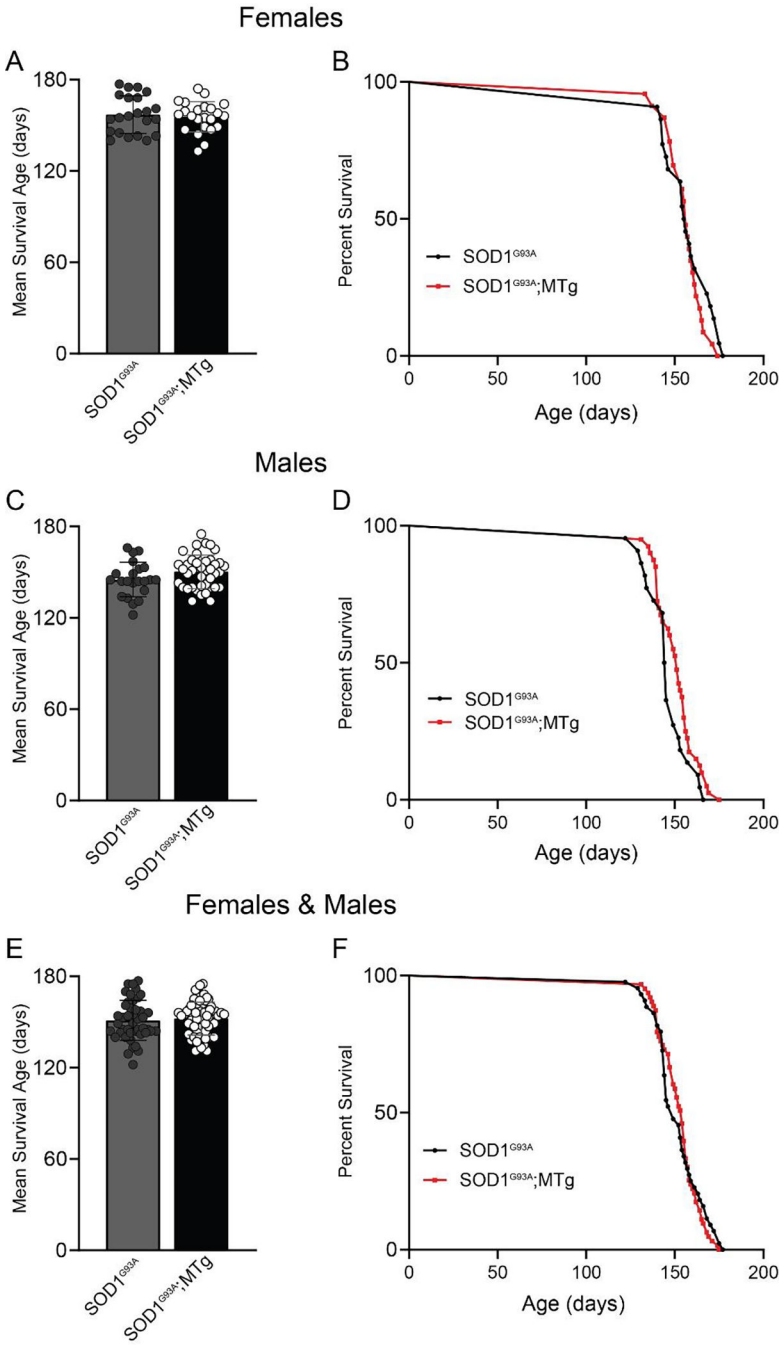

Figure 6.

Increasing KLF15 in muscles does not alter the lifespan of SOD1^{G93A} mice. (A,C,E) Mean survival ages ± S.D of SOD1^{G93A} and SOD1^{G93A};MTg littermates. (B,D,F) Kaplan-Meier survival plots of SOD1^{G93A} and SOD1^{G93A};MTg littermates. (A,B) Female mice, n = 22–23. p = 0.3021, log-rank test. (C,D) Male mice, n = 22–40. p = 0.1025, log-rank test. (E,F) Male and female mice, n = 44–63. p = 0.5641, log-rank test.

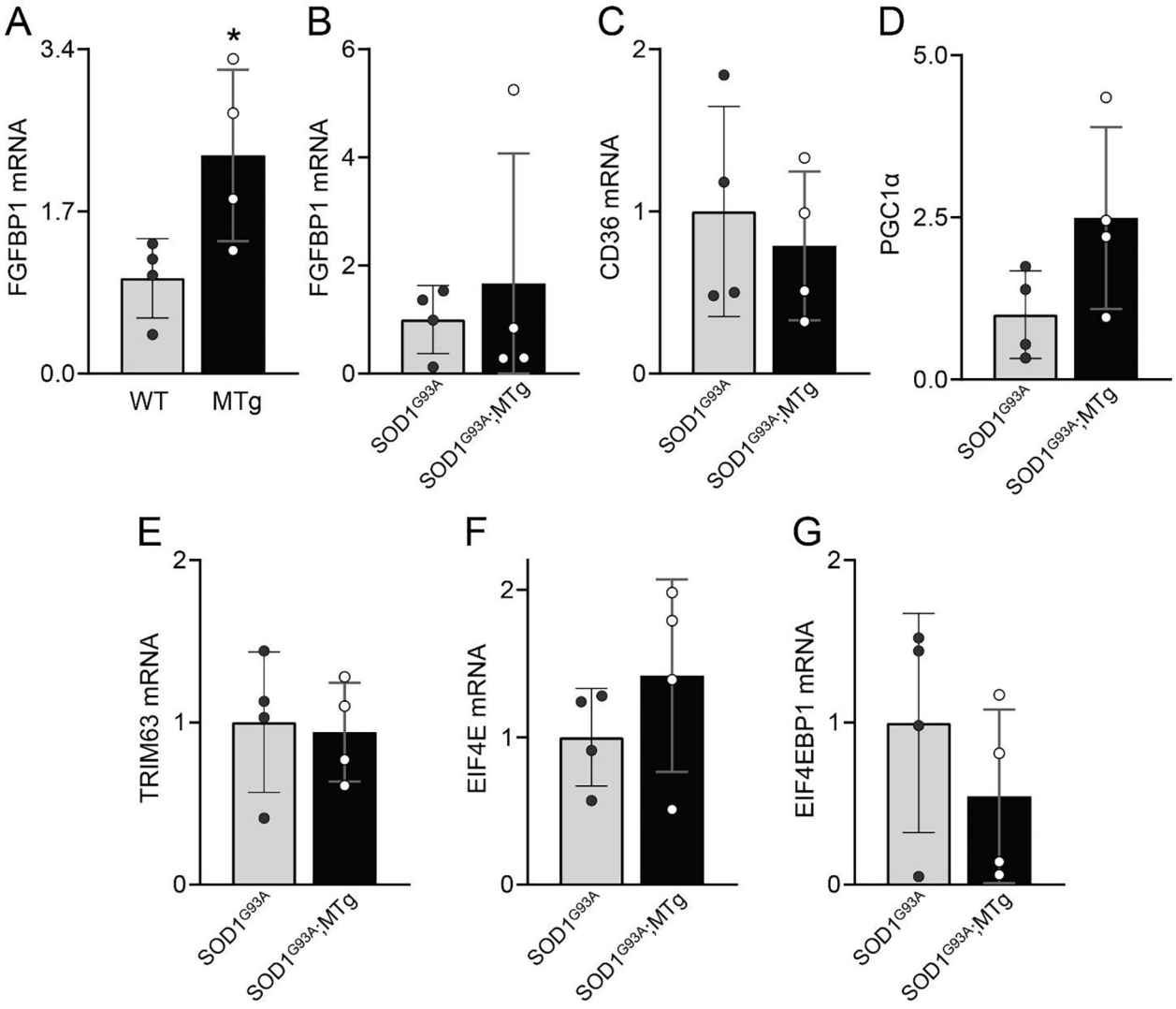

Figure 7.

Transcriptional analysis of TA muscles collected from P90 mice using qPCR. (A) FGFBP1 in WT vs MTg littermates. (B-G) Comparisons between $SOD1^{G93A}$ and $SOD1^{G93A}$;MTg littermates. (B) *FGFBP1*, (C), *CD36*, (D) *PGC1α*, (E) *TRIM63*, (F) *EIF4E*, (G) *EIF4EBP1*. All values reported as mean ± SD; n = 4, * $p < 0.05$.

Table 1.

qPCR primers sequences.

Gene	Forward Primer (5'–3')	Reverse Primer (5'–3')
B2M	TGCTATCCAGAAAACCCCTCAA	GGATTTCAATGTGAGGCGGG
CD36	TTCCTCTGACATTTGCAGGTCT	TGTCTGGATTCTGGAGGGGT
EIF4E	ACTGTGGAACCGGAAACCA	CCCACCTGTTCTGTAGAGGG
EIF4EBP1	AGCCATTCCTGGGGTCACTA	ATTGTGACTCTTCACCGCCTG
FGFBP1	ACACTCACAGAAAGGTGTCCA	CTGAGAACGCCTGAGTAGCC
GAPDH	CCCACTCTTCCACCTTCGATG	GTCCACCACCCTGTTGCTGTAG
KLF15	GCTGGAGGTTTTCCCGCTC	GTGGGAAGCGATGCACTTTG
PGC1α	CCCTGCCATTGTTAAGACC	TGCTGCTGTTCCTGTTTTC
TRIM63	ACAGAG GGTAAAGAAGAACACC	GCGTGTCTCACTCATCTCCTT